ACI STRUCTURAL JOURNAL

A JOURNAL OF THE AMERICAN CONCRETE INSTITUTE

Prepublished Paper

This is a prepublished manuscript. The final manuscript is tentatively scheduled for V. 121, No. 5 and is subject to change.

The DOI for this paper is 10.14359/51740865 and will not change, but won't be activated until the issue has been published.

Evaluation of Flexural Strength and Ductility of Hybrid Prestressed Concrete Members

by W. Nasreddine, A. Obeida, M. Harajli, and H. Nassif

ABSTRACT: *Flexural strength and ductility of exclusively bonded or unbonded steel prestressed concrete (PC) members are well covered and documented in the literature and codes of practice. However, current design methods are limiting the use of hybrid (i.e., a combination of unbonded and bonded steel and Fiber Reinforced Polymer (FRP)) tendons, particularly when using brittle material such as FRP tendons. In this paper, a general procedure for evaluating the nominal moment capacity and ductility of hybrid PC members was developed using strain compatibility approach. The procedure is applicable for members with any combination of bonded or unbonded steel and FRP tendons. Using capacity design approach based on strain compatibility, the ductility performance of several hybrid systems with different parameters were compared. The parameters included, among others, the level of "net tensile strain" in the tension reinforcement at nominal strength adopted in ACI 318-19 as a measure of ductility; concrete compressive strength; and the newly defined hybrid prestressing ratio (HPR). HPR represents the ratio of the moment contribution of the unbonded tendons to the total moment capacity of the member with hybrid tendons. Non-linear analysis was carried out for generating the entire load-deflection and moment-curvature responses of the different systems. The accuracy of the nonlinear analysis was verified by comparing with available experimental data and the analysis results were used to compare traditional curvature ductility measures of the various systems against the ductility measure specified in the ACI Building code. A design example is provided in Appendix A to illustrate the use of the strain compatibility approach.*

Keywords: CFRP; ductility; flexure; hybrid beams; prestressed concrete; strain compatibility; unbonded tendons.

INTRODUCTION AND BACKGROUND

Prestressed concrete (PC) flexural members with hybrid tendons (referred herein as hybrid members) are members prestressed using a combination of bonded and unbonded tendons and/or a combination of different prestressing materials[1]. One application of hybrid members is in the construction of new segmental bridges where precast box segments are post-tensioned together using a combination of internally bonded (grouted) and externally unbonded tendons. Morever, in staged prestressing, pretensioned bridge girders designed for dead and construction loads, are then post-tensioned as composite girder with the deck, using unbonded steel or FRP tendons for full live load. Another application is in the strengthening of existing PC members. Oftentimes, strengthening requires the use of additional internal or external unbonded steel or FRP tendons to increase the members' load carrying capacity. With the evolution of new prestressing material such as non-metallic FRP tendons and new hybrid prestressing systems, the issue of evaluation of the ultimate moment capacity and ductility of these systems has been of particular concern.

The latest ACI Building code[2] has been adopting a new concept for limiting the area of tension reinforcement in reinforced concrete (RC) and conventional bonded or unbonded prestressed concrete (PC) members to achieve a minimum level of ductility. This concept, which was introduced by Mast[3], relies on specifying a minimum "net tensile train" ε_t in the outermost tension reinforcement to be developed in the critical section at nominal flexural strength of the member, excluding strain due to prestressing, creep, shrinkage, and temperature. For reinforced concrete (RC) members, ACI specifies that $\varepsilon_t \geq \varepsilon_{ty} + 0.003$, where ε_{ty} is the yield strain of the steel reinforcement. For RC members with Grade 60 steel, $\varepsilon_t \geq 0.005$. For PC members, ε_{ty} for all types of prestressed reinforcement shall be taken as 0.002 and therefore $\varepsilon_t \geq 0.005$. RC or PC sections satisfying the minimum net tensile strain limit are classified as tension-controlled. Note that for RC or PC sections, the minimum specified limit of $\varepsilon_t \geq 0.005$ is equivalent to specifying a maximum ratio of the neutral axis depth c of the section at ultimate to the depth of reinforcement d_t where ε_t is measured (c/d_t) equal to 0.375. For continuous members, because redistribution of moment depends on the ductility available in the hinge regions, ACI 318-19[2] specifies that redistribution of moment is limited to sections that have a net tensile strain of at least 0.0075 ($c/d_t \leq 0.286$).

Currently, ACI 318-19[2] does not provide guidance for evaluating the ultimate moment capacity and ductility of hybrid PC members. Nonetheless, to design ductile FRP prestressed concrete members, ACI Committee 440[4] introduced the concept of balanced reinforcement ratio ρ_b, which is defined as the ratio at which the strain in the FRP reaches its ultimate strain ε_{fu} simultaneously when the concrete reaches its limiting compressive strain ($\varepsilon_{cu} = 0.003$). The balanced reinforcement ratio is calculated using strain compatibility at nominal flexural strength of the critical section assuming *bonded* PC members with one layer of FRP tendons as follows:

$$\rho_b = 0.85\beta_1 \frac{f_c'}{f_{fu}} \frac{\varepsilon_{cu}}{\varepsilon_{cu} + (\varepsilon_{fu} - \varepsilon_{pef} - \varepsilon_d - \varepsilon_{fr})} \tag{1}$$

Where f'_c is the cylindrical concrete compressive strength; β_1 is concrete strength factor defined in the ACI code; f_{fu} is the ultimate strength of the FRP tendons; ε_{pef} is the effective strain of the tendons after accounting for all prestress losses; ε_d is the decompression strain or strain in concrete at the level of the FRP tendons due to the effective prestressing force; and ε_{fr} is the strain at the level of the tendons due to sustained loads. According to ACI Committee 440[4], ε_d and ε_{fr} can be ignored with no loss of accuracy. Sections with FRP reinforcement ratio $\leq \rho_b$ are expected to fail by rupture of the FRP tendons and hence are classified as tension-controlled, while sections with reinforcement ratio exceeding ρ_b are expected to fail by concrete crushing and hence are referred to as compression-controlled.

In contrast to the ACI Building code, conventional ductility measures proposed in the technical literature are mainly expressed as a ratio of the deformation of the member at ultimate (D_u) to that at yield (D_y), or $\mu_D = D_u/D_y$, where D could be curvature φ, rotation θ, or deflection Δ. The curvature ductility ratio $\mu_{\varphi} = \varphi_u/\varphi_y$ is considered[5] as the building block for quantifying the rotation and deflection ductility ratios. Unfortunately, however, there is no agreement among researchers on the load level at which the ultimate or yield deformation occurs[6], leading to differences in the values of the calculated ductility ratios. Even if researchers agree on the definition of yield and ultimate deformations, conventional ductility ratios are difficult to quantify, particularly when using non-metallic reinforcement such as FRP or high strength steel with no distinct yield point.

Furthermore, the use of ACI Committee 440 concept of balanced reinforcement ratio (Eq. 1) to distinguish between tension-controlled and compression-controlled failure of FRP prestressed concrete sections is deemed irrational and limited in application. For instance, because strain compatibility of PC members with unbonded tendons is member rather than section-dependent, Eq. (1) cannot be applied when unbonded FRP tendon system is used and therefore there is need for an equation which includes unbonded tendons. In addition, linking "tension-controlled" failure, which has been customarily associated with ductile failure, to "rupture" of the FRP tendons is not appreciated by the engineering community. Tension-controlled behavior in accordance with ACI Committee 440 implies "rupture" of the tendons at nominal flexural strength, which could be extremely brittle and sudden and may lead to "collapse" of the entire structural system rather than failure of the tendons only thus negating the whole concept of "ductile" failure. This is particularly true for members prestressed exclusively with FRP tendons.

It appears that the current ACI 318-19[2] concept of linking flexural ductility to the "net tensile strain" that can develop in the outermost tension reinforcement at nominal flexural strength offers a simple and yet rational progressive model for quantifying ductility of all types of concrete structural systems. The authors believe that this ductility concept, which was initially used for RC members and then for conventional PC members, can be easily extended to members prestressed exclusively with FRP tendons or hybrid members prestressed using a combination of bonded and unbonded steel and/or FRP tendons.

RESEARCH SIGNIFICANCE

Current design methods are limiting the use of hybrid tendons. A general strain compatibility approach is developed for evaluating the nominal moment capacity and ductility of hybrid prestressed concrete (PC) members having different combinations of bonded and unbonded tendons and prestressing materials (steel, FRP). Particular attention is devoted to the potential of extending the current ACI's "net tensile strain" concept to cover the design of ductile hybrid PC systems. Non-linear analysis was developed and used to generate the full load-deflection and moment - curvature responses of a variety of hybrid PC members with different strength and reinforcement parameters, and a design example is provided in Appendix A to illustrate the use of the strain compatibility approach.

STRAIN COMPATIBILITY APPROACH

Consider the general case of a prestressed concrete T or I section having a flange width b, a flange thickness h_f, and web width b_w. The prestressed reinforcement at the critical section is assumed for this particular case to consist of bonded steel tendons of area A_{ps} at depth d_p and unbonded FRP tendons of area A_{pfU} at depth d_{pfU} (referred to as hybrid System I). Throughout this paper, the subscript "U" (capital letter) denotes unbonded tendons (steel or FRP) as opposed otherwise to bonded ones, and "f" denotes FRP tendons. Fig. 1(a) shows a hybrid AASHTO type III section used in the design example of Appendix A, while Fig. 1(b) shows the strain distribution across the depth of the section at nominal flexural strength assuming the section fails due to concrete crushing ($\varepsilon_{cu} = 0.003$). The total strains ε_{ps} in the bonded steel and ε_{pfU} in the unbonded FRP tendons at nominal flexural strength are expressed as:

$$\varepsilon_{ps} = \left(\varepsilon_{pa} + \varepsilon_{ce} + \varepsilon_{pe}\right) \tag{2}$$

$$\varepsilon_{pfU} = \left[\Omega\left(\varepsilon_{faU} + \varepsilon_{cefU}\right) + \varepsilon_{pefU}\right] \leq \varepsilon_{fu} \tag{3}$$

From the linear strain distribution across the depth of the section (Fig. 1b):

$$c = \varepsilon_{cu} d_p / (\varepsilon_{pa} + \varepsilon_{cu}) \tag{4}$$

$$\varepsilon_{faU} = (d_{pfU}/d_p)\left(\varepsilon_{pa} + \varepsilon_{cu}\right) - \varepsilon_{cu} \tag{5}$$

The term Ω is a strain reduction factor to account for the slip of the tendons relative to the surrounding concrete (being unbonded); ε_{pa} is the strain in the bonded prestressed steel above concrete decompression at the same level, while ε_{faU} is the "*fictitious strain*" in concrete at the level of the unbonded FRP tendons; $\varepsilon_{pe} = f_{pe}/E_{ps}$ and $\varepsilon_{pefU} = f_{pefU}/E_{pfU}$ where f_{pe} and E_{ps} are the effective prestress and modulus of elasticity of the prestressed steel, while f_{pefU} and E_{pfU} are the those of the unbonded FRP tendons. The terms ε_{ce} and ε_{cefU} are the precompression strains in concrete at the level of the prestressed steel and FRP tendons, respectively:

$$\varepsilon_{ce} = \frac{1}{E_c}\left[\frac{A_{ps} f_{pe}}{A_c} + \frac{A_{ps}\, f_{pe} {e_p}^2}{I_g} + \frac{A_{pfU}\, f_{pefU}}{A_c} + \frac{A_{pfU}\, f_{pefU} e_{fU} e_p}{I_g}\right] \tag{6}$$

$$\varepsilon_{cefU} = \frac{1}{E_c}\left[\frac{A_{pfU} f_{pefU}}{A_c} + \frac{A_{pfU}\, f_{pefU} {e_{fU}}^2}{I_g} + \frac{A_{ps}\, f_{pe}}{A_c} + \frac{A_{ps}\, f_{pe} e_p e_{fU}}{I_g}\right] \tag{7}$$

in which e_p and e_{fU} are the eccentricities of the steel and FRP tendons, respectively; A_c and I_g are the area and moment of inertia of the gross section. Note that ε_{ce} and ε_{cefU} are usually small and hence can be neglected with no loss of accuracy.

It is assumed for generality that the section in Fig. 1a is also reinforced with tension steel A_s (at depth *d*) and compression steel A'_s. Using force equilibrium across the depth of the section assuming T-section behavior (considering average flange thickness for sloping flanges) and that the tension and compression steel yielded:

$$A_{ps} f_{ps} + A_{pfU} E_{pfU}\left[\Omega\left(\varepsilon_{faU} + \varepsilon_{cefU}\right) + \varepsilon_{pefU}\right] + A_s f_y = 0.85 f'_c b_w \beta_1 c + 0.85 f'_c (b - b_w) h_f + A'_s f_y$$

(8)

Replacing the values of c and ε_{faU} from Eqs. (4) and (5) into Eq. (8) and expressing ε_{pa} as a function ε_{ps} (Eq. 2) leads to the general strain compatibility relationship between the stress f_{ps} and strain ε_{ps} of the bonded prestressed tendons at nominal flexural strength given in Eq. (Ia) of Table 1. The solution for f_{ps} and corresponding ε_{ps} is obtained as the intersection point between Eq. (Ia) and the material stress-strain curve of the prestressed steel which, in the absence of experimental data, can be generated using available constitutive stress-strain models. Neglecting the contribution of the compression steel A'_s, the nominal moment capacity M_n is calculated as:

$$M_n = A_{ps}f_{ps}\left(d_p - d_o\right) + A_{pfU}f_{pfU}\left(d_{pfU} - d_o\right) + A_s f_y (d - d_o) \tag{9}$$

where f_{pfU} is given in Eq. (Ib) of Table 1 and d_o is the distance from the centroid of the concrete compression force to the outermost concrete compression fiber. For the general case of a T section behavior ($\beta_1 c > h_f$):

$$d_o = \frac{\frac{(b-b_w)h_f^2}{2} + b_w(\beta_1 c)^2/2}{b_w\beta_1 c + (b-b_w)h_f} \tag{10}$$

For rectangular section behavior $b_w = b$, and hence $d_o = \beta_1 c/2$.

Assuming the bonded prestressed steel is the outermost tension reinforcement (i.e., $d_t = d_p$, neglecting the presence of ordinary tension steel), the maximum reinforcement or ductility requirement to produce tension-controlled section is then satisfied when Eq. (Ic) in Table 1 is satisfied.

Using the above procedure (Eqs. 2 through 10), similar approaches can be derived for other hybrid systems including systems with *bonded steel-unbonded steel* tendons (System II), *bonded FRP-unbonded steel* tendons (System III), and *bonded FRP-unbonded FRP* tendons (system IV). A summary of these expressions is provided in Table 1. It should be mentioned that the compatibility equations derived for System I can be easily adapted to hybrid systems with *bonded steel – bonded FRP* tendons (not shown for brevity) by setting $\Omega = 1.0$ and substituting instead the terms A_{pf}, d_{pf}, ε_{cef}, ε_{pef}, e_f, and E_{pf} corresponding to those of the bonded FRP tendons. Note that in deriving the compatibility equation for System II it is assumed, *for simplification,* that the strain and corresponding stress f_{psU} in the unbonded steel tendons at nominal strength seldom exceeds the linear elastic range of the material stress-strain curve[2, 7]; that is, $f_{psU} \leq 0.9 f_{pyU}$, where f_{pyU} is the yield strength of the unbonded tendons. Note also that for exclusively unbonded systems, ACI 318-19 requires that a minimum area of ordinary tension steel A_s equal to $0.004 A_{ct}$ be provided for crack control, where A_{ct} is the area between the tension face and the neutral axis of the gross section. Therefore, it is customary that for exclusively unbonded members with either steel or FRP tendons, the net tensile strain ε_t is measured at the depth d of the ordinary steel, which is normally the outermost tension reinforcement ($d_t = d$).

Strain Reduction Factor Ω

In broad terms, the strain reduction factor Ω is equal to the ratio of the equivalent length of the plastic region L_p in the beam divided by the length of the tendons between anchorages (or simply the span length) L. The value of L_p depends mainly on the type of load application and span-to-depth ratio of the member. Several experimentally derived expressions are available in the technical literature for estimating L_p of unbonded PC members[7-11]. A summary of these expressions is reported by Harajli[7]. For the purpose of this study, the equivalent plastic hinge length of hybrid members (and hence Ω) is estimated based on the experimental study of Corley[12] and the recommendation of Mattock[13] regarding the results, leading to the following expression[8]:

$$\Omega = L_p/L = 0.95/f + d/L + 0.05 \tag{11}$$

Where $d =$ depth of the tension reinforcement (can be taken equal to the depth d_t of the outermost tension reinforcement where ε_t is measured); and $f = 6.0$, 3.0, or ∞ for uniformly distributed load, 2 - 1/3 point load, and single concentrated load, respectively. It should be mentioned that for uniformly distributed load, which is the most common type of load application, the term Ω (Eq. 11) varies only slightly between 0.275 for members with span-to-depth ratio (d_t/L) of 15 to 0.237 for span-to-depth ratio of 35. Therefore, it would be reasonable to adopt a constant value of $\Omega = 0.25$ regardless of the span-to-depth ratio with no loss of accuracy. Note that the values of Ω calculated using Eq. (11) are only slightly higher than the values derived by Naaman and Alkhairi[9], and significantly lower than the values recommended by Lee et al.[10] It should be indicated that other expressions of Ω were tried and the difference in the results was deemed insignificant.

NON-LINEAR ANALYSIS OF HYBRID PC MEMBERS

The nonlinear analysis procedure used in this study is based on the incremental deformation method used earlier[14-16] for evaluating the nonlinear flexural behavior of bonded or unbonded PC members when subjected to monotonically increasing load to failure. The analysis requires the use of relationships for the stress-strain behavior of the constituent materials, which are typically obtained through constitutive empirical models.

The stress-strain (f_c - ε_c) relationship of concrete in compression used in this study is that proposed by Popovics[17]. This equation is expressed as follows:

$$f_c = f'_c \frac{\varepsilon_c}{\varepsilon'_c} \frac{n}{n-1+(\varepsilon_c/\varepsilon'_c)^n} \tag{12}$$

Where: $n = 0.4x10^{-3} f'_c(psi) + 1$, and $\varepsilon'_c = (2.7x10^{-4}) \sqrt[4]{f'_c(psi)}$.

The stress-strain relationship $(f_{ps} - \varepsilon_{ps})$ of the prestressed steel is modelled using the following equation developed by Menegotto and Pinto[18]:

$$f_{ps} = E_{ps}\varepsilon_{ps}\left[Q + \frac{1-Q}{\left[1+\left(\frac{E_{ps}\varepsilon_{ps}}{Kf_{py}}\right)^{N}\right]^{1/N}}\right] \leq f_{pu} \tag{13}$$

Where typical values of K, N, Q, E_{ps}, and f_{py}, and f_{pu} were developed by Naaman[19] for various types and grades of the prestressed steel. For Grade 270, 7-wire strands used in this study, the corresponding values are equal, respectively, to 1.0618, 7.344, 0.01174, 27900 ksi (192371 MPa), 243.5 ksi (1679 MPa), and 278 ksi (1917 MPa), with ultimate strain ε_{pu} not exceeding 0.069.

The FRP tendons exhibit a linear stress-strain ($f_{pf} - \varepsilon_{pf}$) behavior until rupture. Unless otherwise derived directly from test data, the typical properties of carbon FRP (CFRP) tendons used in this study are assumed to be those of Tokyo rope tendon, with an ultimate stress f_{fu} of 370 ksi (2550 MPa), a modulus of elasticity E_{pf} of 21750 ksi (150 GPa), and an ultimate strain ε_{fu} of 1.7%. Typical stress-strain relationships of the prestressed reinforcement are presented in Fig. 2.

Whenever accounted for in the analysis, a bilinear relationship composed of elastic and strain-hardening portions is used to model the stress-strain curve of reinforcing steel bars. The modulus of elasticity E_s was taken equal to 29000 ksi (2x10^5 MPa), and the ratio of the strain hardening modulus E_{sh} to the elastic modulus E_s was taken equal to 0.005.

In the nonlinear analysis, the member is subdivided into small beam elements. The concrete strain at top fiber of the critical midspan section is increased in small increments to simulate a gradual increase in the applied load. At each strain level, the strains and stresses in the reinforcement and the member deflection or section curvature are obtained using a multi-iteration procedure for achieving compatibility of deformations along the length of the member, and equilibrium of forces across the depth of all beam elements. The strain in the top fiber is increased until failure occurs. For CFRP prestressed members, failure may develop due to concrete crushing or due to CFRP tendon rupture, whichever occurs first. Failure of concrete is assumed, *conservatively*, to take place when the compressive strain reaches $\varepsilon_{cu} = 0.003$.

Analysis Validation

The accuracy of the non-linear analysis is verified by comparing with test data reported in the technical literature. The data correspond to beam specimens prestressed using bonded steel tendons (Specimens PP2S2 and PP1S3) tested by Harajli[20]; bonded CFRP tendons (R-4-0.5-H) tested by Abdelrahman[21]; unbonded steel tendons (B3 and B18) and hybrid bonded-unbonded steel tendons (B25) tested by Ozkul et al.[22] Also, beams specimens prestressed using unbonded CFRP tendons (RO55) tested by Heo et al.[23]; and bonded steel-unbonded CFRP tendons (B-1) tested by Jererett et al.[24], and (PG11) tested by Ghallab et al.[25] Design details and material properties of the specimens are reported in the respective references. Comparisons of the analytical and experimental load versus deflection response, moment versus curvature response, and moment versus increase in tendon stress above effective prestress, Δf_{psU}, for the various specimens are provided in Fig. 3.

It can be seen in Figs. 3 that, despite little discrepancies at different levels of applied load, a very good agreement exists between the analytical and test results, which is in clear support of the accuracy of the non-linear analysis method.

PARAMETRIC EVALUATION

For the purpose of parametric evaluation, several beams in each of the four hybrid PC systems of Table 1 were designed using “capacity design” approach based on strain compatibility and then analyzed for evaluating their deformation capacity or ductility by generating their load-deformation behavior using the method of nonlinear analysis developed in this study. The “design” approach involves calculating different combinations of areas of hybrid prestressed reinforcement for a given PC section required to achieve the same nominal moment capacity corresponding to specific levels of net tensile strain $\varepsilon_t \geq 0.005$. The design approach is described briefly below:

For a given PC section to be designed using a combination of, say, bonded steel and unbonded CFRP tendons (System I), a desired level of ε_t at the outermost tension reinforcement is first selected. Using this net tensile strain, and assuming flexural failure occurs by concrete crushing, the neutral axis depth c and the total strain in each of the hybrid reinforcement can be calculated using Eqs. (2) through (5). The stresses in the prestressed reinforcement can thus be calculated using the stress-strain relationship of the prestressing material (steel and/or CFRP) assumed identical to that used in the nonlinear analysis (Eq. 13). In order to evaluate different hybrid systems or combinations of areas of bonded and unbonded prestressed reinforcement, a Hybrid Prestressing Ratio (*HPR*) parameter is introduced in this study. This parameter is defined as the ratio of the moment contribution of the unbonded prestressed tendons to the moment contribution of the combined bonded and unbonded tendons, as follows:

$$HPR = \frac{A_{pfU} f_{pfU}(d_{pfU} - d_o)}{A_{ps} f_{ps}(d_p - d_o) + A_{pfU} f_{pfU}(d_{pfU} - d_o)} \tag{14}$$

where d_o is given in Eq. (10). A value of *HPR* = 0.0 corresponds to members prestressed with exclusively bonded steel *or* bonded CFRP tendons, while *HPR* = 1.0 corresponds to members with unbonded tendons (either steel *or* CFRP). By selecting a value of *HPR* (between 0 and 1), the areas of the hybrid prestressed reinforcement A_{ps} and A_{pfU} can be calculated (for the selected ε_t) by solving simultaneously Eq. (14) and Eq. (8) (i.e., by solving two equations with two unknowns). Note that the terminology used in Eq. (14) corresponds to beams in System I, but the same *HPR* concept and "design" procedure can be applied for beams with any combination of hybrid reinforcement in Systems II through IV of Table 1.

A simply supported beam with rectangular section, having a span length L = 360 in. (9.1 m), and subjected to a uniformly distributed load was used to carry out the parametric evaluation. The section has a width b = 12 in. (305 mm), and height h = 24 in. (610 mm). The depths of the unbonded and bonded reinforcement throughout the length of the beam were assumed both equal to $0.85h$ or 20.4 in. (518 mm). For comparative purposes, the size of the section and the depth of the prestressed reinforcement were selected identical to those used by Naaman et al.[6] The parameters evaluated included the value of ε_t mobilized at nominal strength ($\varepsilon_t = 0.005, 0.0075, 0.01, 0.015$) to produce different ductility levels; concrete strength f'_c of 6.0 ksi (41.4 MPa) and 10 ksi (69 MPa); and the Hybrid Prestressing Ratio HPR (0.0, 0.33, 0.66, and 1.0). For every selected level of ε_t, the areas of the prestressed reinforcement were calculated using the above-described procedure of capacity design corresponding to each of the four values of *HPR*. According to ACI Committee 440[4], the effective stress in the CFRP tendons should be limited to between 40 and 65 *percent* of their ultimate strength due to stress-rupture limitations. In this study, the effective prestress was taken as $0.50f_{pu}$ and $0.45f_{fu}$ for the steel and CFRP tendons, respectively.

Design results are summarized in Table 2. It should be emphasized that the capacity design approach is only used in this study for the purpose of parametric evaluation. In other words, it is not intended to substitute the traditional method of service load design by which the areas of the prestressed reinforcement are estimated such that concrete allowable stresses specified in ACI 318-19[2] are satisfied. Therefore, in using this design approach, it is tacitly assumed that the size of the section, the calculated areas of the hybrid reinforcement, and the magnitudes of the applied service loads lead to concrete stresses that satisfy the allowable concrete tension and compression stress requirements of ACI 318-19[2].

The beams in each of the systems in Table 2 were analyzed using the method of non-linear analysis developed in this study by generating and comparing their load (or midspan moment) versus midspan deflection response and moment versus curvature response at the critical midspan section. In addition, the ultimate stresses in the prestressed reinforcement and nominal flexural strength of the different beams generated using non-linear analysis were compared with those calculated using strain compatibility approach. Figures 4 - 7 show representative results for the four different systems corresponding to f'_c of 6 ksi (41.4 MPa) and 10 ksi (69 MPa), respectively. The last four columns in Table 2 show ratios of nominal flexural strength calculated using strain compatibility to that predicted using nonlinear analysis for all beams in the various hybrid systems.

Discussion of Results

Flexural failure of all beams in Systems I and II occurred by concrete crushing at the limiting concrete compressive strain ε_{cu} of 0.003. It can be seen from Figs. 4(a) and 5(a) that the nominal load/moment capacity of the beams in Systems I or II with different *HPR* and for a selected level of ε_t were practically the same as originally anticipated. Also, except for minor differences, the deformations (curvatures and deflections) mobilized at nominal flexural strength were also consistently similar for all values of *HPR* and at all values of ε_t.

However, as shown in Figs. 6(a) and 7(a), the beams in Systems III and IV in which *bonded* CFRP tendons are used (beams with *HPR* = 0, 0.33, and 0.66) failed prematurely due to rupture of the tendons (at $\varepsilon_t = 0.009$ and $\varepsilon_c = 0.0025$) before reaching the desired net tensile strain of 0.01, and also prior to concrete crushing. Therefore, because CFRP is a brittle material, the maximum net tensile strain $\varepsilon_{t(\max)}$ that can develop in bonded CFRP tendons is controlled by the magnitude of the ultimate tensile strain ε_{fu} and the level of the effective prestrain ε_{pef} of the tendons ($\varepsilon_{t(\max)} = \varepsilon_{fu} - \varepsilon_{pef} - \varepsilon_{cef}$). Consequently, in designing PC members with *bonded* CFRP tendons, in order to avoid sudden and brittle failure associated with tendons rupture, it is recommended that the members be designed such that flexural failure occurs by concrete crushing before tendon rupture. Neglecting the small precompression strain ε_{cef}, this can be achieved by limiting the desired net tensile strain in the tendons such that $\varepsilon_t \leq (C_s\varepsilon_{fu} - \varepsilon_{pef})$, where C_s is FRP "ultimate strain reduction factor" which may be taken between 0.9 and 0.95 as deemed appropriate by code authorities. Alternatively, this last requirement is equally satisfied by requiring that $c/d_t \geq [\varepsilon_{cu}/(\varepsilon_{cu} + C_s\varepsilon_{fu} - \varepsilon_{pef})]$. Note that when *unbonded* CFRP tendons are used, because of slip of the tendons relative to the surrounding concrete (which is compensated for by using a strain reduction factor Ω), the total strain in the tendons at nominal flexural strength was considerably lower than the rupture strain ε_{fu} regardless of the value of the desired ε_t.

Furthermore, Figs. 4(b) – 7(b) show that there is a reasonably good agreement (within ±10 *percent* and mostly within ± 5 *percent*) between the nonlinear analysis predictions of ultimate stresses in the prestressed reinforcement (bonded/unbonded steel or CFRP) and those predicted using strain compatibility approach. It should be indicated that the relatively larger scatter in the predictions of the ultimate stress for the unbonded tendons (steel or CFRP) when compared to the bonded ones is attributed to the inherent scatter in predicting the stress in unbonded tendons at ultimate[6], which is mainly due to the difficulty in quantifying accurately the strain reduction factor Ω. Also, as shown in the last four columns of Table 2 and the statistical data provided, excellent agreement exists between the nominal moment capacities M_n estimated using strain compatibility approach and those calculated using nonlinear analysis.

In order to verify the applicability of the "net tensile strain" concept to other types of sections, the same rectangular beam used earlier was re-designed using instead a T section. The section has a flange width b = 48 in. (1220 mm), flange thickness h_f = 3 in. (76 mm), web width b_w = 12 in. (305 mm), overall height $h = 24$ in. (610 mm), and depths of hybrid reinforcement of 20.4 in. (518 mm). The section was designed considering only one hybrid system (System I) corresponding to *bonded steel* - *unbonded CFRP* tendons (design results are not shown for brevity). Nonlinear analysis results of the moment-curvature behavior of this section for different concrete compressive strengths are shown in Fig. 8. It can be seen that the trend of results are consistently similar to those generated for the rectangular section, indicating that the net tensile strain concept for evaluating ductility is independent of the type of section.

One of the most important observations in Figs. 4(a) through 7(a) and Fig. 8 is that although the moment-curvature responses of the beams in the various systems for a selected ε_t may have significantly different shapes, all beams (excluding those which experienced premature failure by rupture of the bonded CFRP tendons) were able to attain the same curvature at nominal flexural strength. Therefore, all of these beams give the same degree of warning prior to failure which is in support of the observation made by Mast[3].

COMPARISON OF NET TENSILE STRAIN VERSUS CONVENTIONAL DUCTILITY MEASURES

The results of the non-linear analysis were used to compare traditional curvature ductility measures of the beams in the various systems against the ductility measure specified in the ACI Building code. Fig. 9 shows variations of the ultimate curvature φ_u and curvature ductility ratio $\mu_\varphi = \varphi_u/\varphi_y$ versus c/d_t for the hybrid rectangular beams (Systems I through IV in Table 2) and for the T beams (System I) evaluated in this study. The curvature φ_u is measured at the peak load of the moment-curvature response (Figs. 4a – 7a) while the yield curvature φ_y is measured, customarily and for consistency, when the strain in the outermost prestressed reinforcement above decompression reaches ε_{ty} which for PC members is equal to 0.002 (ACI 318-19[2]). Note that, as mentioned earlier, there is a direct correlation between c/d_t and the net tensile strain [$c/d_t =$

$\varepsilon_{cu}/(\varepsilon_{cu}+\varepsilon_t)$]. When flexural failure occurs by concrete crushing ($\varepsilon_{cu} = 0.003$), the minimum value of $\varepsilon_t \geq 0.005$ corresponds to a maximum value of $c/d_t \leq 0.375$.

It can be seen in Fig. 9 that a consistent relation exists between the ultimate curvature φ_u as well as the curvature ductility ratio φ_u/φ_y and c/d_t (or ε_t) for all parameters and hybrid systems evaluated in the current investigation. At the minimum level of ε_t of 0.005 (c/d_t = 0.375), a curvature ductility of at least 2.0 is available. For ε_t = 0.0075 (c/d_t = 0.286), which is the minimum ductility limit specified in ACI 318-19[2] for moment redistribution in continuous members, a curvature ductility between 3.0 and 4.0 can be available. Also, for low values of c/d_t, except when flexural failure occurs due to CFRP tendon rupture (when bonded CFRP tendons are used), a curvature ductility in excess of 7.0 can be attained. Furthermore, despite failing prematurely due to rupture of the bonded CFRP tendons the beams in Systems III and IV (shown in circle in Fig. 9) were able to mobilize a reasonably large ε_t of 0.009 (c/d_t of 0.217) which is translated into a curvature ductility of approximately 4.0. Note that since the net tensile strain ε_t at rupture of the bonded CFRP tendons is equal to ("$\varepsilon_{fu} - \varepsilon_{pef} - \varepsilon_{cef}$"), it may vary for a given ε_{fu} of the CFRP material depending on the design effective prestress f_{pef} of the tendons.

Shown also in Fig. 9 are relevant results represented by dashed and solid lines generated from a study undertaken by Naaman et al.[6] In that study, a comprehensive parametric evaluation using nonlinear analysis was carried out for quantifying the curvature ductility ratio of partially prestressed concrete members, i.e., members with a combination of bonded prestressed steel and ordinary reinforcing steel. The parameters included type of section (rectangular, flanged), reinforcing index ω [$\omega = (A_{ps}f_{ps} + A_s f_y - A'_s f_y)/bd_p f'_c$], partial prestressing ratio PPR [$PPR = A_{ps}f_{ps}/(A_{ps}f_{ps} + A_s f_y)$], concrete strength f'_c, grade of the prestressed steel, effective prestress f_{pe}, and ratio of compression steel. It was concluded that the reinforcing index ω (or

c/d) is an excellent independent variable to describe flexural ductility because it encompasses the effect of several other variables such as the reinforcement ratio, partial prestressing ratio, concrete compressive strength, and type of section. Based on the results of that study, three equations were derived for quantifying curvature ductility of partially prestressed sections as a function ω (which can also be expressed as a function of c/d) depending on the values of the design parameters (*PPR*, f_{pe}, and f'_c) used, namely an upper bound, an average, and a lower bound.

The results represented by the dashed lines in Fig. 9 correspond to a particular case when the rectangular section is prestressed exclusively with Grade 270 bonded steel tendons (*PPR* = 1.0 or $A_s = 0$) and having $f_{pe} = 0.5f_{pu}$ (Naaman et al.[6]); that is, similar to the section in System I with *HPR* = 0.0 analyzed in the current study. The results represented by the solid lines (Fig. 9) correspond to the *lower bound* variations generated by Naaman et al. which are also applicable for the range of values of the design parameters used in the current investigation (high concrete compressive strength, fully prestressed members ($A_s = 0.0$ or *PPR* = 1.0), and low effective prestress ($f_{pe} = 0.5f_{pu}$)). It can be seen in Fig. 9 that, despite differences in the definition of the "yield" and "ultimate" points on the moment-curvature response between the current study and that of Naaman et al.[6], a very good agreement is observed between the results of the two studies, which supports the use of ε_t or c/d_t as a rational indicator of the ductility level available in all types of concrete structural systems, including the hybrid PC systems under investigation.

CONCLUSIONS

Based on the results of this study the following conclusions are drawn:

1. The strain compatibility approach generated in this study could serve as a very powerful and accurate tool for evaluating the flexural strength and ductility of hybrid PC members.

2. The “net tensile strain” ε_t specified in the ACI Building code (or alternatively the ratio of the neutral axis depth c at ultimate to the depth d_t of the outermost tension reinforcement, c/d_t) is a unifying parameter for evaluating ductility of flexural concrete members, including hybrid PC members under evaluation.

3. Hybrid systems prestressed with a combination of bonded steel and *unbonded* steel or CFRP tendons (Systems I and II) are likely to fail by concrete crushing and are able to mobilize a considerably larger ε_t than the minimum of 0.005 specified in the ACI Building code. On the other hand, hybrid systems in which *bonded* CFRP tendons are used (Systems III and IV) may fail prematurely due to rupture of the CFRP tendons before concrete crushing, thus limiting the value of ε_t or ductility that can be achieved when compared with beams with unbonded CFRP tendons.

4. In designing members involving the use of bonded CFRP tendons, to avoid brittle failure due to tendons rupture, particularly when using exclusively bonded CFRP tendons, it is recommended that the members be designed such that flexural failure occurs due to concrete crushing before the tendons reach their rupture strain ε_{fu}. This can be achieved by requiring that $\varepsilon_t \leq (C_s\varepsilon_{fu} - \varepsilon_{pef})$, or equivalently $c/d_t \geq [\varepsilon_{cu}/(\varepsilon_{cu} + C_s\varepsilon_{fu} - \varepsilon_{pef})]$, where C_s is FRP ultimate strain reduction factor, which may be selected between 0.9 and 0.95 as deemed appropriate by code authorities.

5. A consistent relation exists between the ultimate curvature/curvature ductility ratio and ε_t (or c/d_t) for all hybrid systems evaluated in this study. This agrees well with the ductility trends of conventional PC systems reported earlier in the technical literature. At the minimum net tensile strain of 0.005 (c/d_t = 0.375) all hybrid systems were able to develop a minimum curvature ductility ratio $\mu_\varphi = \varphi_u/\varphi_y$ of 2.0. For ε_t= 0.0075 (c/d_t = 0.286), which is the minimum ductility limit specified in ACI 318-19[2] for moment redistribution in continuous members, μ_φ between 3.0 and 4.0 can be available.

6. Despite failing by tendon rupture, all beams in Systems III and IV, in which bonded CFRP tendons are used, were able to mobilize an ε_t of 0.009 and a reasonably good μ_φ of about 4.0 before rupture of the tendons. On the other hand, at values of $\varepsilon_t > 0.018$ or $c/d_t < 0.14$, all beams in Systems I and II, in which bonded steel and unbonded steel/CFRP tendons are used, were able to mobilize a μ_φ in excess of 7.0.

A design example is provided in Appendix A to illustrate the use of the developed strain compatibility approach.

AUTHOR BIOS

*ACI Member **Wassim Nasreddine** is a Research Associate at Rutgers University. His research interests include prestressed concrete member behavior, innovative concrete materials, strengthening and retrofitting of concrete structures.*

*ACI Member **Adi Obeidah** is a Structural Engineer with HNTB. He received his B.S. and M.S. from American University of Sharjah, and PhD from Rutgers University. His research focuses on prestressed fiber reinforced concrete and UHPC behavior with non-metallic reinforcement, strengthening and retrofitting of concrete elements.*

***Mohamed Harajli** is a Professor of civil engineering at the American University of Beirut (AUB). His research interests include design and behavior of reinforced, prestressed, and fiber reinforced concrete members; and seismic repair and strengthening of concrete structures.*

***Hani Nassif,** FACI, is a Professor of structural engineering at Rutgers University. He is a past member of ACI's Technical Activity Committee (TAC). He currently serves on ACI Committee 435, Deflection of Concrete Building Structures; and 343, Bridge Design. His research focuses on structural concrete and the use of advanced cementitious and composite materials.*

ACKNOWLEDGEMENTS

Support received in part from the Connected Cities for Smart Mobility toward Accessible and Resilient Transportation (C2SMART) Tier I University Transportation Center at New York University and the New Jersey Department of Transportation (NJDOT) through the Bridge Resource Program (BRP) is gratefully appreciated. The contents of this paper do not reflect the official views or policies of the supporting agencies. The accuracy and facts of the data presented herein are the responsibility of the authors.

REFERENCES

1. Obeidah, A., and Nassif, H., “Serviceability of Beams Prestressed with Hybrid (Steel/ Carbon Fiber-Reinforced Polymer) Tendons,” *ACI Struct. J.*, V. 119, No. 3, May 2022, pp.179-190.

2. ACI Committee 318, “Building Code Requirements for Structural Concrete (ACI 318-19) and Commentary (ACI 318-19R),” *American Concrete Institute*, 2019, Farmington Hills, MI, 624 pp.

3. Mast, R. F., “Unified Design Provisions for Reinforced and Prestressed Concrete Flexural and Compression Members,” *ACI Structural Journal*, 89(2), 1992, pp. 185-199.

4. ACI Committee 440.4R-04, “Prestressing Concrete Structures with FRP Tendons,” *American Concrete Institute*, 2004, Farmington Hills, MI,

5. Park, R., and Paulay, T., ”Reinforced Concrete Structures,” John Wiley & Sons, 1975, Wiley-Interscience.

6. Naaman, A. E.; Harajli, M. H.; and Wight, J. K., "Analysis of Ductility in Partially Prestressed Flexural Members," *Journal of the Prestressed Concrete Institute* , Vol. 31, No. 3, May-June, 1986, pp. 64-87.

7. Harajli M., “On the Stress in Unbonded Tendons at Ultimate: Critical Assessment and Proposed Changes,” *ACI Structural Journal*, V. 103, No. 6, Nov.-Dec. 2006, pp.803-812.

8. Harajli, M. H., “Effect of Span-Depth Ratio on the Ultimate Steel Stress in Unbonded Prestressed Concrete Members,” *ACI Structural Journal*, V. 87, No. 3, May-June 1990, pp. 305-312

9. Naaman, A. E., and Alkhairi, F. M., “Stress at Ultimate in Unbonded Post-Tensioned Tendons: Part 2-Proposed Methodology,” *ACI Structural Journal*, V. 88, No. 6, Nov.-Dec. 1991 pp 683-692.

10. Lee, L., Moon, J., and Lim, J., “Proposed Methodology for Computing of Unbonded Tendon Stress at Flexural Failure,” *ACI Structural Journal*, V. 96, No. 6, Nov.-Dec. 1999, pp.1040-1048.

11. Tam, A., Pannell, F. N., “The Ultimate Moment Resistance of Unbonded Partially Prestressed Reinforced Concrete Beams”. *Magazine of Concrete Research*, (Wexham Springs), V. 28, No. 97, Dec. 1976, pp. 203-208.

12. Corley, W. G., "Rotational Capacity of Reinforced Concrete Beams," Proceedings, *ASCE, Structural Division*, V. 92, No. ST5, October 1966, pp. 121-146, also PCA Bulletin 17108.

13. Mattock, A. H., “Discussion of "Rotational Capacity of Reinforced Concrete Beams," by W. Corley, *proceedings*, ASCE, Vol. 93, ST2, April 1967, pp. 519-522. https://doi.org/10.1061/JSDEAG.0001678

14. Harajli M., and Hijazi S., “Evaluation of the Ultimate Steel Stress in Partially Prestressed Concrete Beams,” *PCI Journal*, Vol. 36, No. 2, January-February 1991, pp.62-82.

15. Moon, J. H., and Burns, N. H., “Flexural Behavior of Member with Unbonded Tendons II: Applications,” *Journal of Structural Engineering*, Vol. 123, No. 8, August 1997.

16. Harajli M.; Khairallah N.; and Nassif H., “Externally Prestressed Members: Evaluation of Second-Order Effects,” *Journal of Structural Engineering,* Vol. 125, No. 10, 1999, ASCE, ISSN 0733-9445/99/0010-1151–1161.

17. Popovics S., “A Numerical Approach to the Complete Stress-Strain Curve of Concrete,” *Cement and Concrete Research*, Vol. 3, 1973, pp. 583-599.

18. Menegotto, M., and Pinto, P. E., “Method of Analysis for Cyclically Loaded R.C. Plane Flames,” *IABSE* Preliminary Report for Symposium on Resistance and Ultimate Deformability of Structures acted on Well-Defined repeated Loads, Lisbon, Portugal, 1973, pp. 15-22.

19. Naaman, A. E., “An Approximate Nonlinear Design Procedure for Partially Prestressed Concrete Beams,” Computers and Structures, Vol. 17, No. 2, 1983, pp. 287-293.

20. Harajli, M. H., "*Deformation and Cracking of Partially Prestressed Concrete Beams Under Static and Cyclic Fatigue Loading,"* Dissertation Presented at the University of Michigan in Partial Fulfillment for the Requirements of Doctor of Philosophy, 1985, 387 pp.

21. Abdelrahman, A. A., “Serviceability of Concrete Beams Prestressed by Fibre Reinforced Plastic Tendons,” *PhD Thesis*, Department of Civil and Geological Engineering, University of Manitoba, Winnipeg, Manitoba, 1995.

22. Ozkul, O.; Nassif, H.; Tanchan, P.; and Harajli, M., “Rational Approach for Predicting Stress in Beams with Unbonded Tendons,” *ACI Structural Journal,* V. 105, No. 3, May-June 2008, pp. 338-347.

23. Heo, S.; Shin, S; and Lee C., “Flexural Behavior of Concrete Beams Internally Prestressed with Unbonded Carbon Fiber-Reinforced Polymer Tendons,” *Journal of Composites for Construction*, ASCE, March-April 2013.

24. Jerrett C.V., and Ahmad S.H., "Behavior of Prestressed Concrete Strengthened by External FRP Post-Tensioned Tendons," *Advanced Composite Materials in Bridges and Structures*, Canadian Society for Civil Engineering, 1996, Montreal, Quebec.

25. Ghallab A., and Beeby A.W., "Behaviour of PSC Beams Strengthened by Unbonded Parafil Ropes," FRPRCS-5; fibre-reinforced plastics for reinforced concrete structures, 2001, pp. 671-680.

APPENDIX A - DESIGN EXAMPLE

Simply supported post-tensioned girders with AASHTO Type III section shown in Fig. 1(a) were used to support the floor slab of a warehouse. Span length = 70 ft. The prestressed reinforcement is to consist of a combination of bonded prestressed steel and unbonded CFRP tendons. The load is uniformly distributed and the girder is to be designed using *Class U* (uncracked member) in accordance with ACI classification.

Section properties: Self-weight $w_g = 0.583$ k/ft (8.5 kN/m); cross section area $A_c = 560$ in.^{2} (361290 mm^2); moment of inertia $I_g = 125390$ in.^{4} (5.2x10^{10} mm^4); distance from neutral axis (NA) to the bottom and top fibers are $y_b = 20.27$ in. (515 mm), and $y_t = 24.73$ in. (628 mm), respectively; section modulus relative to the bottom fiber $S_b = 6186$ in^3 (101.4x10^6 mm^3), and that relative to the top fiber $S_t = 5070$ in^3 (83.1x10^6 mm^3); $d_p = 42$ in. (1069 mm) [$e_{ps} = 17.3$ in. (439 mm)]; $d_{pfU} = 40$ in. (1016 mm) [$e_{pfU} =$ 15.3 in. (389 mm)].

Applied midspan moments: Moment due to: self-weight $M_g = 4285$ k-in (485.4 kN-m); slab weight $M_s = 4000$ k-in (453.2 kN-m); superimposed dead load $M_{sup} = 2000$ k-in (226.6 kN-m); and live load $M_L = 5000$ k-in (566.4 kN-m).

Material properties: Concrete compressive strength at transfer of the prestressing force $f'_{ci} = 4.5$ ksi (31 MPa), and $f'_c = 6.0$ ksi (41.4 MPa). The prestressed steel consists of ½ in. – 7 wire strands Grade 270 ($f_{pu} = 1862$ MPa) having $E_{ps} = 27900$ ksi (192370 MPa). The CFRP tendons consist of 0.6 in. (15.2 mm) in diameter 7-strands [area per one strand = 0.179 in.^{2} (115.5 mm^2)] and having E_{pfU} =21750 ksi (150,000 MPa), f_{fu} = 370 ksi (2550 MPa), and ε_{fu} = 0.017. Stress in the prestressed steel at transfer of the prestressing force $f_{pi} = 0.65 f_{pu}$, $f_{pe} = 0.54 f_{pu}$. Effective stress in the CFRP tendons $f_{pefU} = 0.45 f_{fu}$

It is required to design the hybrid girder such that the critical midspan section satisfies the allowable concrete stresses, and also the ultimate flexural strength and maximum reinforcement/ductility requirements of the ACI Building code

Service Load Design

It is assumed that the girder is post-tensioned (precast) using bonded prestressing steel with an effective prestressing force $F_{pe} = A_{ps} f_{pe}$ such that it balances the applied midspan moment due to self-weight of the girder after accounting for all prestress losses. Therefore: $F_{pe} = M_g/e_{ps}$ = 247.7 kip (1104.5 kN), and A_{ps} = 1.7 in.^{2} 1097 mm^2).

Use 11 ½ in. -7 wire strands with actual total area A_{ps} = 1.68 in.^{2} (1085 mm^2), and F_{pe} = 245.0 kip (1092.5 kN).

By balancing the applied midspan moment due to the girder's self-weight, the concrete service compression stresses at the top and bottom fiber of the girder at the midspan section are both equal to F_{pe}/A_c = 0.44 ksi (3.0 MPa) which is significantly less than ACI's allowable concrete compression stress of $0.6 f'_c$ = 3.6 ksi (24.8 MPa). Note that the concrete compression stress in the bottom and top fiber of the section immediately after transfer of the prestressing force ($f_{pi} = 0.65 f_{pu}$), would be equal to 0.65 ksi (4.5 MPa) and 0.37 ksi (2.6 MPa), respectively, both of which are less than the allowable stress of $0.6 f'_{ci} =$ 2.7 ksi (18.6 MPa).

The girder is transported to the site and the slab was cast using non-composite construction with shores provided to support the weight of the slab during casting (shored construction). At this stage, the girder is assumed to have acquired its full concrete compressive strength of 6.0 ksi (41.4 MPa). The girder is then prestressed with additional unbonded CFRP tendons having a depth of 40 in. (1016 mm) at midspan to resist the additional moments due to slab load, superimposed dead load, and live load.

Considering ACI's concrete allowable stresses at service (compression stress under full service load ≤ $0.6f'_c$, compression stress under sustained load ≤ $0.45f'_c$, and tension stress ≤ $6\sqrt{f'_c}$), and considering the combined effect of the prestressed steel and CFRP tendons leads to a design effective prestressing force in the CFRP tendons $F_{pefU} = A_{pfU}f_{pefU}$ ≥ 198 kips, with the allowable concrete tension stress at the bottom fiber controlling the design. This leads to $A_{pfU} = F_{pefU}/f_{pefU}$ = 1.2 in.^{2} (774 mm^2).

Use 7 CFRP strands leading to an actual area A_{pfU} = 1.25 in.^{2} (806 mm^2), and F_{pefU} = 208 kip (927.5 kN).

Flexural Strength and Ductility Analysis

Using Eq. (Ia) of Table 1 by assuming rectangular section behavior ($b_w = b$), and substituting the values of $A_s = A'_s = 0.0$; $\Omega = 0.25$; $\varepsilon_{pe} = f_{pe}/E_{ps} = 0.0052$; $\varepsilon_{pefU} = f_{pefU}/E_{pfU} = 0.0077$; $\varepsilon_{ce}(Eq.6) = 0.00042$; and $\varepsilon_{cefU}(Eq.7) = 0.00039$, leads to:

$$f_{ps} = 4.59/(\varepsilon_{ps} - 0.0026) - 3851.6\varepsilon_{ps} - 103.4$$

The intersection point between the compatibility equation and the stress - strain curve of the prestressing steel (using the one adopted in this study as expressed in Eq. 13) leads to: $f_{ps} = 259$ ksi (1785 MPa) and $\varepsilon_{ps} = 0.0137$. Consequently, $\varepsilon_{pa}(Eq.\ 2) = 0.0081$; $\varepsilon_{faU}(Eq.5) = 0.0076$; $\varepsilon_{pfU}(Eq.3) = 0.0096$; hence $f_{pfU} = E_{pfU}\varepsilon_{pfU} = 208.8$ ksi (1440 MPa).

Using equilibrium of forces across the depth of the section ($Eq.$ 8) leads to a depth of the concrete stress block $a = 8.5$ in. (217 mm). By idealizing the size of the flange as having an average constant thickness $h_f = 9.25$ in. (260 mm) implies that $a < h_f$ and therefore the section behaves as a rectangular section as initially assumed.

$M_n(Eq.9) = 25757.0$ k-in (2918 kN-m)

The net tensile strain $\varepsilon_t = \varepsilon_{pa} = 0.0081 > 0.005$, which implies that the section is tension-controlled, and hence the strength reduction factor $\varphi = 0.9$. As such $M_u = \varphi M_n = 23181.0$ k-in (2626 kN-m) $>$ $[1.2(M_g + M_s + M_{sup}) + 1.6M_L] = 19412.0$ k-in (2199 kN-m), and therefore the section satisfies the ultimate flexural strength requirements of ACI 318-19.

Assuming the CFRP tendons are bonded (for the sake of comparison), the design and analysis procedures above would still apply in exactly the same manner, except that for flexural analysis the value of Ω is set equal to 1.0. The reader can verify that the behavior is a T section behavior with the following summary of the strain compatibility results: $f_{ps}(Eq.Ia) = [2.0/(\varepsilon_{ps} - 0.0026) - 15373.8\varepsilon_{ps} + 210.7]$; $f_{ps} = 254$ ksi (1751 MPa); $\varepsilon_{ps} = 0.0116$, $\varepsilon_{pa} = 0.0064$; $c = 13.4$ in. (340 mm) and $a = \beta_1 c = 10.1$ in. (257 mm); $\varepsilon_{fa} = 0.0057$; $\varepsilon_{pf} = 0.0138 < \varepsilon_{fu} = 0.017$; and $f_{pf} = E_{pf}\varepsilon_{pf} = 300$ ksi (2069 MPa); $\varepsilon_t = \varepsilon_{pa} = 0.0064 > 0.005$, which implies that the section is, once again, classified as tension-controlled and hence $\varphi = 0.9$; $M_u = \varphi M_n = 26231.0$ k-in (2972 kN-m) $> [1.2(M_g + M_s + M_{sup}) + 1.6M_L] =$ 19412.0 k-in (2199 kN-m).

Note that the use of unbonded CFRP tendons resulted in larger ductility, but smaller ultimate moment capacity as would be expected (by about 13 *percent*) when compared to bonded tendons.

List of Illustrations

Table 1 – Summary of compatibility equations for different hybrid PC systems

Table 2 - Design results of the hybrid beams/systems used in the parametric evaluation (*1 in. = 25.4 mm, 1 ksi = 6.895 MPa)*

Fig. 1 – (a) AASHTO Type III hybrid PC section used in the design example of Appendix A; (b) strain distribution at nominal flexural strength (all dimensions are in inches - 1 in. = 25.4 mm).

Fig. 2 – Material models for the prestressing steel and CFRP tendons used in the nonlinear analysis.

Fig. 3 – Comparison of nonlinear analysis with experimental results (1 kip = 4.46 kN, 1 ksi = 6.895 MPa, 1 in. = 25.4 mm).

Fig. 4 (a) – Moment versus curvature and moment versus deflection behavior generated using nonlinear analysis for the beams in System I (1 in. = 25.4 mm; 1 kip = 4.46 kN).

Fig. 4 (b) –Nonlinear analysis versus strain compatibility results of the ultimate stress f_p (f_{ps}/f_{pfU}) for the beams in System I (1 ksi = 6.895 MPa).

Fig. 5 – (a) Representative moment-curvature behavior; (b) nonlinear analysis versus strain compatibility results of the ultimate stress f_p (f_{ps}/f_{psU}) for the beams in System II (1 in. = 25.4 mm, 1 kip = 4.46 kN, 1 ksi = 6.895 MPa).

Fig. 6 – (a) Representative moment-curvature behavior; (b) nonlinear analysis versus strain compatibility results of the ultimate stress f_p (f_{pf}/f_{psU}) for the beams in System III (1 in. = 25.4 mm, 1 kip = 4.46 kN, 1 ksi = 6.895 MPa).

Fig. 7 – (a) Representative moment-curvature behavior; (b) nonlinear analysis versus strain compatibility results of the ultimate stress f_p (f_{pf}/f_{pfU}) for the beams in System IV (1 in. = 25.4 mm, 1 kip = 4.46 kN, 1 ksi = 6.895 MPa).

Fig. 8 – Moment – curvature behavior generated using nonlinear analysis for the beams with a T section in System I (1 in. = 25.4 mm; 1 kip = 6.895 MPa).

Fig. 9 – Variation of (a) ultimate curvature, and (b) curvature ductility ratio versus c/d_t for the designed beams in hybrid systems I through IV (1 in. = 25.4 mm).

Table 1 – Summary of compatibility equations for different hybrid PC systems

PC System	Compatibility Equations
I – (*Bonded Steel - Unbonded FRP*)	$f_{ps} = \frac{1}{A_{ps}}\frac{0.85\beta_1 f'_c b_w \varepsilon_{cu} d_p}{(\varepsilon_{ps}-\varepsilon_{pe}-\varepsilon_{ce}+\varepsilon_{cu})} - \frac{A_{pfU}}{A_{ps}}E_{pfU}\left[\Omega[(\varepsilon_{ps}-\varepsilon_{pe}-\varepsilon_{ce}+\varepsilon_{cu})\frac{d_{pfU}}{d_p}-\varepsilon_{cu}+\varepsilon_{cefU}]+\varepsilon_{pefU}\right] + \frac{A'_s f_y - A_s f_y + 0.85 f'_c(b-b_w)h_f}{A_{ps}}$ (Ia) $f_{pfU} = E_{pfU}\left[\Omega\left(\varepsilon_{faU}+\varepsilon_{cefU}\right)+\varepsilon_{pefU}\right]$ (Ib) $\varepsilon_t = \varepsilon_{pa} = \varepsilon_{cu}\,(d_p - c)/c \geq 0.005$ (Ic) c = Eq. (4)
II – (*Bonded Steel -Unbonded Steel*)	$f_{ps} = \frac{1}{A_{ps}}\frac{0.85\beta_1 f'_c b_w \varepsilon_{cu} d_p}{(\varepsilon_{ps}-\varepsilon_{pe}-\varepsilon_{ce}+\varepsilon_{cu})} - \frac{A_{psU}}{A_{ps}}E_{psU}\left[\Omega[(\varepsilon_{ps}-\varepsilon_{pe}-\varepsilon_{ce}+\varepsilon_{cu})\frac{d_{pU}}{d_p}-\varepsilon_{cu}+\varepsilon_{ceU}]+\varepsilon_{peU}\right] + \frac{A'_s f_y - A_s f_y + 0.85 f'_c(b-b_w)h_f}{A_{ps}}$ (IIa) $f_{psU} = E_{psU}\left[\Omega\left(\varepsilon_{paU}+\varepsilon_{ceU}\right)+\varepsilon_{peU}\right] \leq 0.9 f_{pyU}$ (IIb) $\varepsilon_{paU} = \frac{d_{pU}}{d_p}\left(\varepsilon_{pa}+\varepsilon_{cu}\right)-\varepsilon_{cu}$ (IIc) ε_t (Eq. Ic)
III – (*Bonded FRP -Unbonded Steel*)	$c = [\sqrt{(k_2{}^2 + 4k_1k_3)} - k_2]/2k_1$ (IIIa) Where: $k_1 = 0.85\beta_1 f'_c b_w$ $k_2 = 0.85 f'_c(b-b_w)h_f + A'_s f_y - A_s f_y - A_{pf}E_{pf}\left(\varepsilon_{cef}+\varepsilon_{pef}-\varepsilon_{cu}\right) - A_{psU}E_{psU}\left[\Omega(\varepsilon_{ceU} - \varepsilon_{cu}) + \varepsilon_{peU}\right]$ $k_3 = (A_{pf}E_{pf}d_{pf} + \Omega A_{psU}E_{psU}d_{pU})\varepsilon_{cu}$ $f_{pf} = E_{pf}\left[\varepsilon_{cu}\left(d_{pf}-c\right)/c + \varepsilon_{cef} + \varepsilon_{pef}\right] \leq f_{fu}$ (IIIb) $f_{psU} = \Omega E_{psU}\left[\varepsilon_{cu}(d_{pU}-c)/c + \varepsilon_{ceU}\right] + E_{psU}\varepsilon_{peU}$ (IIIc) $\varepsilon_t = \varepsilon_{fa} = \varepsilon_{cu}\,(d_t = d_{pf} - c)/c \geq 0.005$ (IIId)
IV – (*Bonded FRP - Unbonded FRP*)	Same as for System III, except that the area A_{psU}, depth d_{pU}, pre-compression strain ε_{ceU}, effective strain ε_{peU}, and modulus of elasticity E_{psU} corresponding to the unbonded steel tendons are replaced respectively by A_{pfU}, d_{pfU}, ε_{cefU}, ε_{pefU} and E_{pfU} corresponding to the unbonded FRP tendons.

Table 2 - Design results of the hybrid beams/systems used in the parametric evaluation *(1 in. = 25.4 mm, 1 ksi = 6.895 MPa)*

Hybrid Systems			System I		System II		System III		System IV		$\frac{M_n(Strain\ Compatibility)}{M_n\ (Non-Linear\ Analysis)}$			
			Bonded Steel - Unbonded CFRP		Bonded Steel - Unbonded Steel		Bonded CFRP - Unbonded Steel		Bonded CFRP - Unbonded CFRP		**Hybrid System**			
f'_c	ε_t	*HPR*	A_{ps} (in^2)	A_{pfU} (in^2)	A_{ps} (in^2)	A_{psU} (in^2)	A_{pf} (in^2)	A_{psU} (in^2)	A_{pf} (in^2)	A_{pfU} (in^2)	**I**	**II**	**III**	**IV**
f'_c = 6 ksi	0.005	0	1.44	0.00	1.44	0.00	1.28	0	1.28	0.00	0.98	0.98	0.96	0.96
		0.33	0.96	0.60	0.96	0.67	0.85	0.66	0.85	0.60	0.97	0.96	0.95	0.95
		0.66	0.48	1.20	0.48	1.34	0.43	1.33	0.43	1.20	0.98	0.98	0.96	0.96
		1	0.00	1.62	0.00	1.81	0.00	1.8	0.00	1.62	0.99	0.99	1.00	0.99
	0.0075	0	1.05	0.00	1.05	0.00	0.81	0	0.81	0.00	0.99	0.99	0.96	0.96
		0.33	0.70	0.43	0.70	0.47	0.54	0.46	0.54	0.43	0.98	0.98	0.94	0.94
		0.66	0.35	0.85	0.35	0.93	0.27	0.92	0.27	0.85	0.99	0.99	0.96	0.95
		1	0.00	1.11	0.00	1.22	0.00	1.2	0.00	1.11	1.01	1.02	1.03	1.01
	0.01*	0	0.83	0.00	0.83	0.00	0.56	0	0.56	0.00	0.99	0.99	1.00	1.00
		0.33	0.56	0.32	0.56	0.35	0.38	0.34	0.38	0.32	0.99	0.99	0.97	0.97
		0.66	0.28	0.64	0.28	0.70	0.19	0.68	0.19	0.64	1.01	1.02	1.00	0.98
		1	0.00	0.81	0.00	0.88	0.00	0.85	0.00	0.81	1.02	1.04	1.01	1.00
	0.015	0	0.60	0.00	0.60	0.00	Failure occurred by CFRP rupture at ε_t = 0.009				0.99	0.99		
		0.33	0.40	0.21	0.40	0.22					1.00	0.98		
		0.66	0.20	0.41	0.20	0.45					1.03	0.99		
		1	0.00	0.48	0.00	0.53					1.03	0.98		
f'_c = 10 ksi	0.005	0	2.08	0.00	2.08	0.00	1.84	0	1.84	0.00	0.97	0.97	0.95	0.95
		0.33	1.39	0.87	1.39	0.97	1.23	0.96	1.23	0.87	0.97	0.96	0.94	0.95
		0.66	0.69	1.73	0.69	1.94	0.61	1.92	0.61	1.73	0.97	0.97	0.96	0.95
		1	0.00	2.42	0.00	2.71	0.00	2.69	0.00	2.42	1.00	0.99	1.00	1.00
	0.0075	0	1.51	0.00	1.51	0.00	1.17	0	1.17	0.00	0.99	0.99	0.95	0.95
		0.33	1.01	0.61	1.01	0.67	0.78	0.66	0.78	0.61	0.98	0.98	0.94	0.93
		0.66	0.50	1.23	0.50	1.35	0.39	1.33	0.39	1.23	0.99	1.00	0.94	0.95
		1	0.00	1.68	0.00	1.84	0.00	1.81	0.00	1.68	1.01	1.01	1.02	1.01
	0.01*	0	1.20	0.00	1.20	0.00	0.81	0	0.81	0.00	0.99	0.99	1.01	1.01
		0.33	0.80	0.46	0.80	0.50	0.54	0.49	0.54	0.46	0.99	0.99	0.98	0.97
		0.66	0.40	0.93	0.40	1.01	0.27	0.98	0.27	0.93	1.00	1.01	1.01	0.98
		1	0.00	1.24	0.00	1.34	0.00	1.3	0.00	1.24	1.02	1.03	1.01	0.99
	0.015	0	0.86	0.00	0.86	0.00	Failure occurred by CFRP rupture at ε_t = 0.009				0.99	0.99		
		0.33	0.57	0.30	0.57	0.32					1.00	0.98		
		0.66	0.29	0.59	0.29	0.65					1.03	0.98		
		1	0.00	0.75	0.00	0.83					1.04	0.98		
										Average	1.00	0.99	0.98	0.97
										Std Dev.	0.02	0.02	0.03	0.02
										Minimum	0.97	0.96	0.94	0.93
										Maximum	1.04	1.04	1.03	1.01

- L = 360 in.; b = 12 in..; h = 24 in.
- Steel Tendon: E_{ps} = 27890 ksi; f_{pu} = 278 ksi; f_{py} = 243.5 ksi; ϵ_{pu} = 0.069; f_{pe} = 0.5f_{pu}
- CFRP Tendon: E_{pf} = 21750 ksi; f_{fu} = 370 ksi; ϵ_{fu} = 0.017; f_{pfe} = 0.45f_{fu}
- Reinforcing Steel: A_s = 0.58 in.^{2} for beams with *HPR* = 1.0; A_s = 0.0 in.^{2} otherwise
- Depth of prestressed steel/CFRP or reinforcing steel = 0.85h = 20.4 in.

(*) The bonded CFRP tendons in Systems III and IV ruptured at $\varepsilon_t = 0.009$

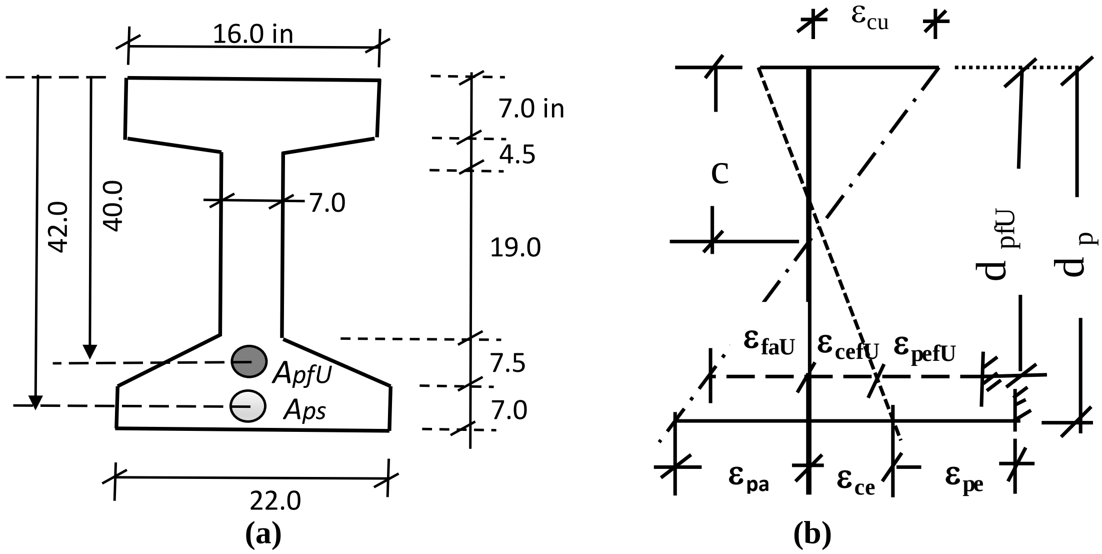

Fig. 1 – (a) AASHTO Type III hybrid PC section used in the design example of Appendix A; (b) strain distribution at nominal flexural strength (all dimensions are in inches - 1 in. = 25.4 mm).

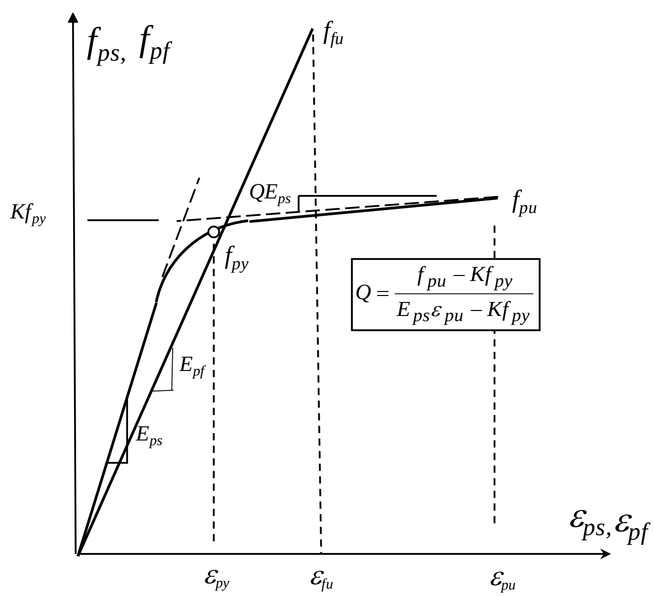

Fig. 2 – Material models for the prestressing steel and CFRP tendons used in the nonlinear analysis.

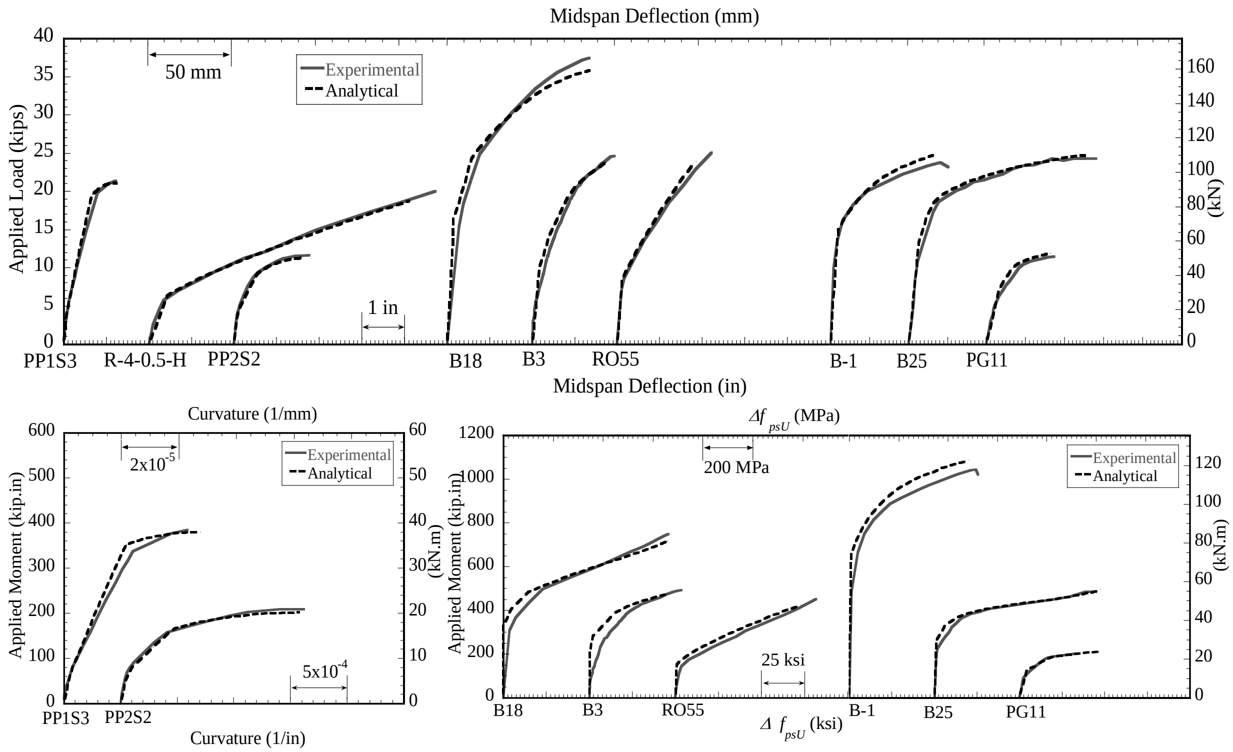

Fig. 3 – Comparison of nonlinear analysis with experimental results (1 kip = 4.46 kN, 1 ksi = 6.895 MPa, 1 in. = 25.4 mm).

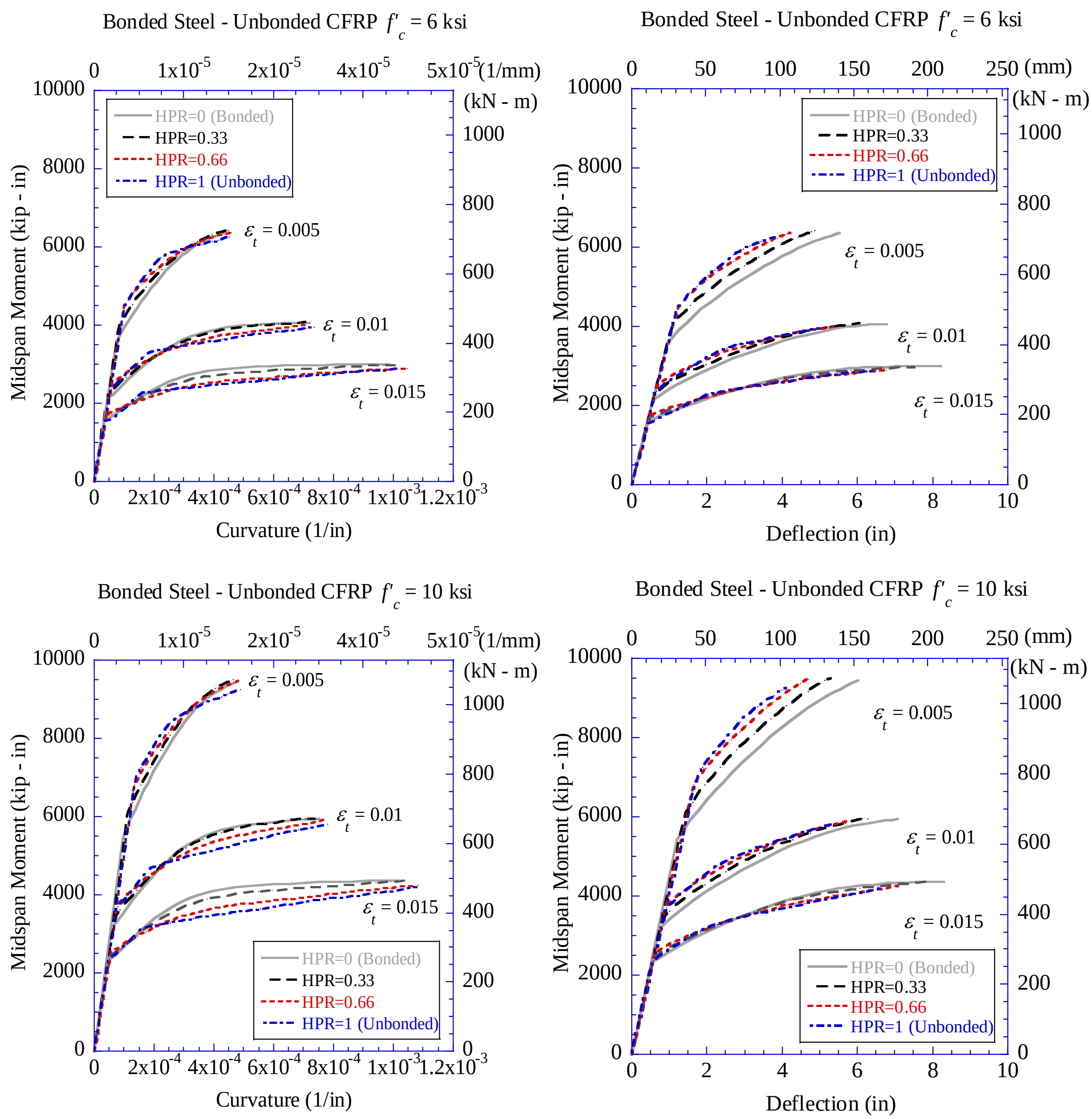

Fig. 4 (a) – Moment versus curvature and moment versus deflection behavior generated using nonlinear analysis for the beams in System I (1 in. = 25.4 mm; 1 kip = 4.46 kN).

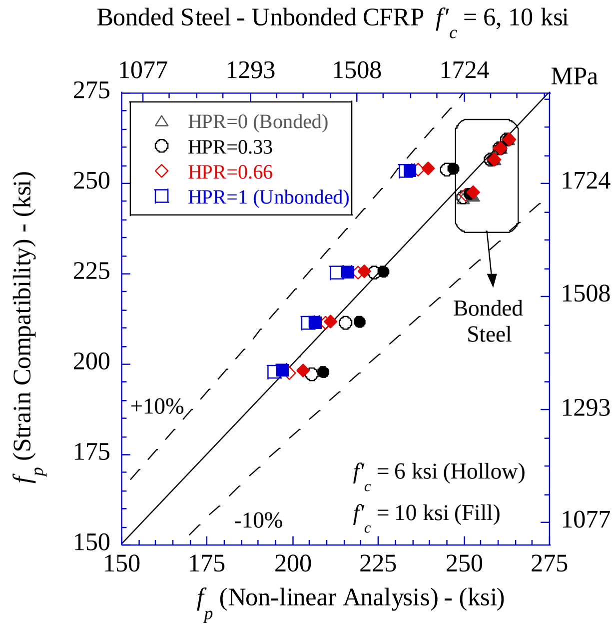

Fig. 4(b) –Nonlinear analysis versus strain compatibility results of the ultimate stress f_p (f_{ps}/f_{pfU}) for the beams in System I (1 ksi = 6.895 MPa).

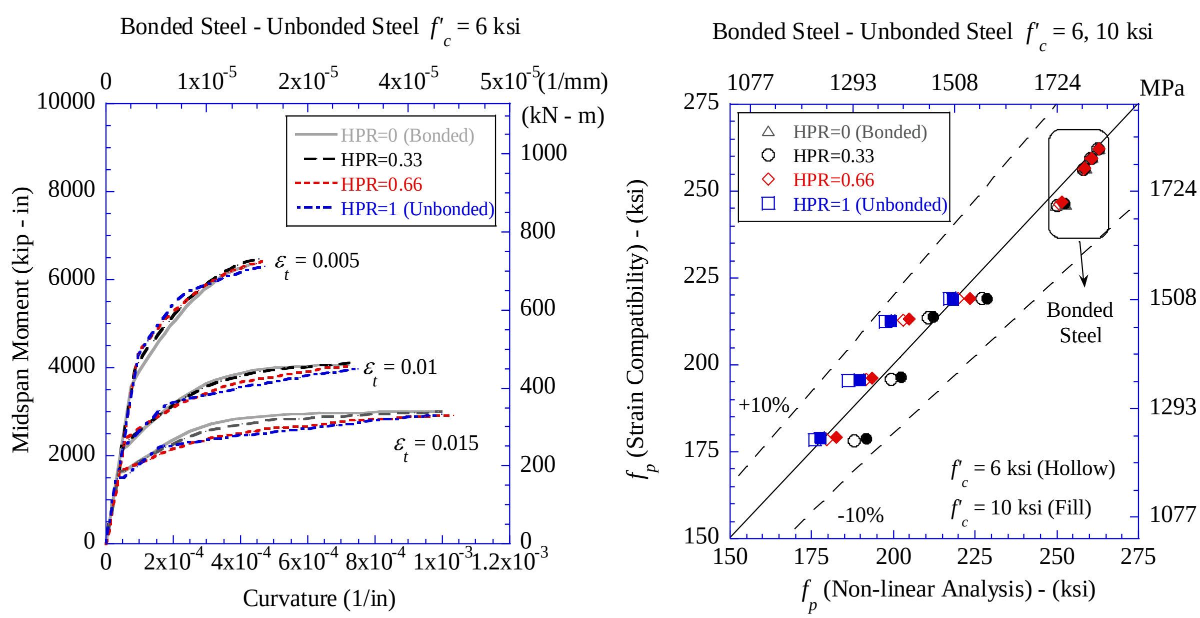

(a) (b)

Fig. 5 – (a) Representative moment-curvature behavior; (b) nonlinear analysis versus strain compatibility results of the ultimate stress f_p (f_{ps}/f_{psU}) for the beams in System II (1 in. = 25.4 mm, 1 kip = 4.46 kN, 1 ksi = 6.895 MPa).

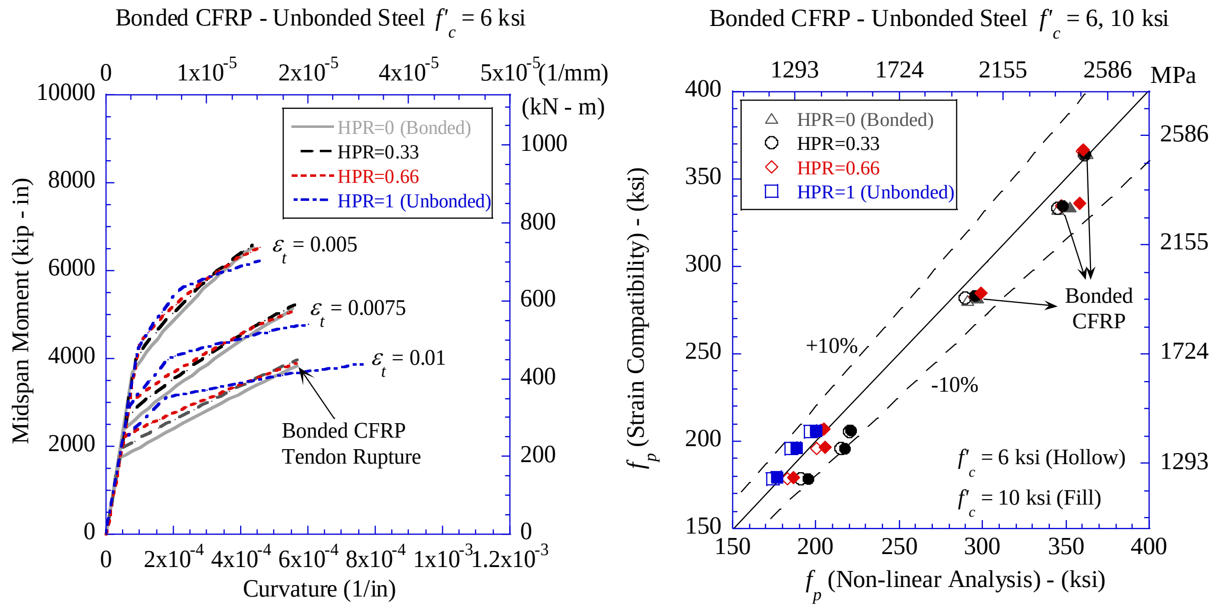

(a) (b)

Fig. 6 – (a) Representative moment-curvature behavior; (b) nonlinear analysis versus strain compatibility results of the ultimate stress f_p $(f_{pf}\,/f_{psU})$ for the beams in System III (1 in. = 25.4 mm, 1 kip = 4.46 kN, 1 ksi = 6.895 MPa).

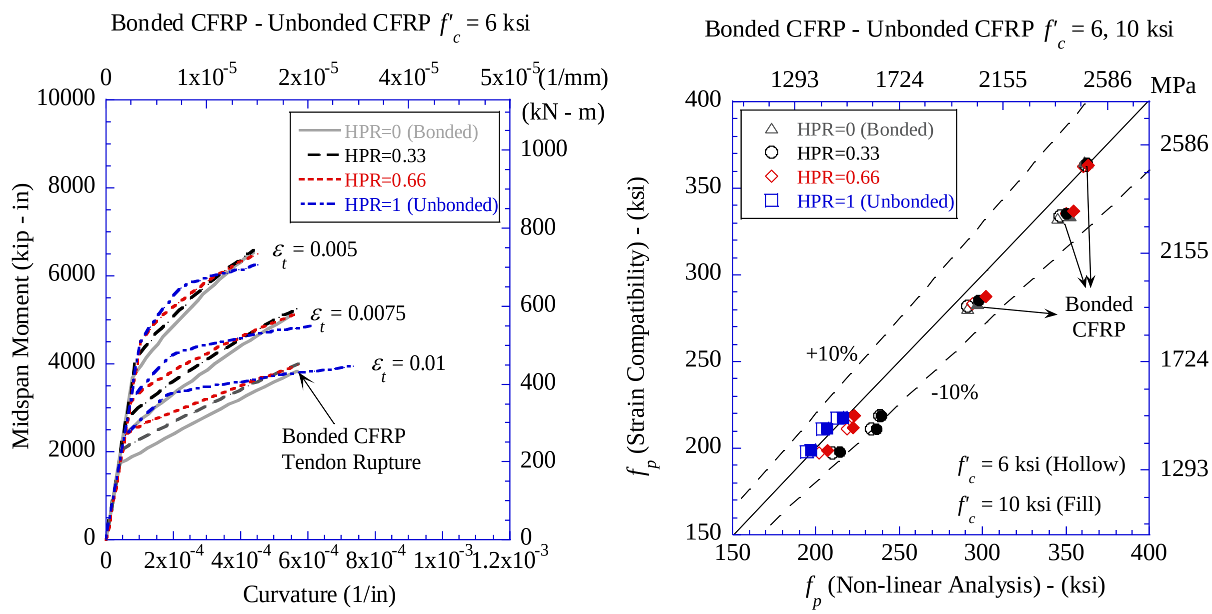

(a) (b)

Fig. 7 – (a) Representative moment-curvature behavior; (b) nonlinear analysis versus strain compatibility results of the ultimate stress f_p $(f_{pf}\,/f_{pfU})$ for the beams in System IV (1 in. = 25.4 mm, 1 kip = 4.46 kN, 1 ksi = 6.895 MPa).

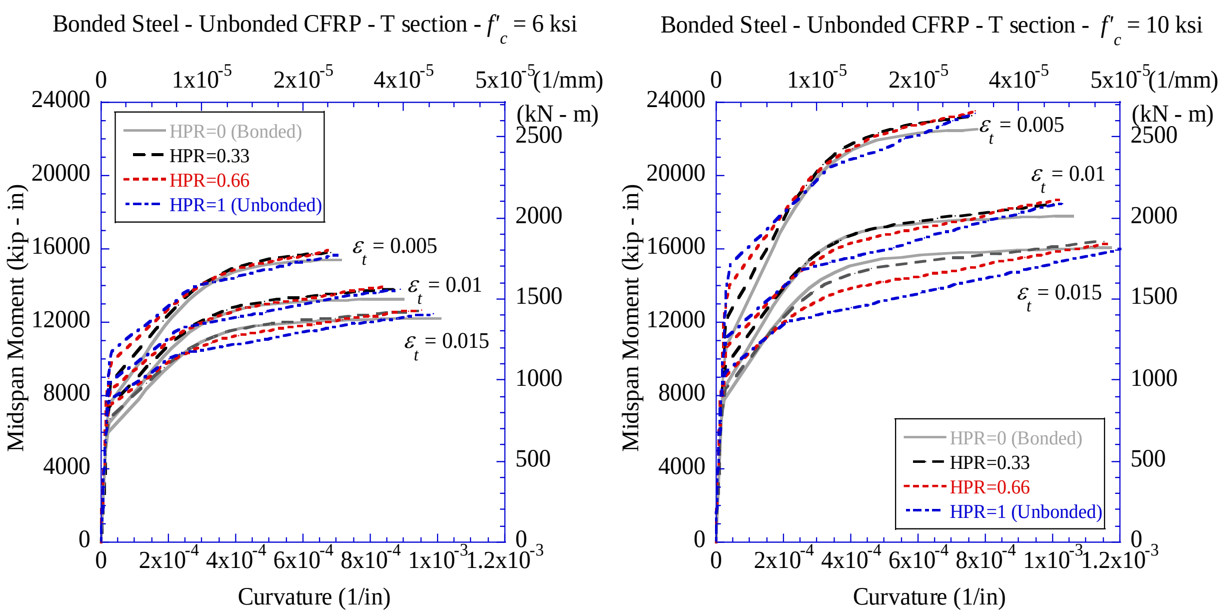

Fig. 8 – Moment – curvature behavior generated using nonlinear analysis for the beams with a T section in System I (1 in. = 25.4 mm; 1 kip = 6.895 MPa).

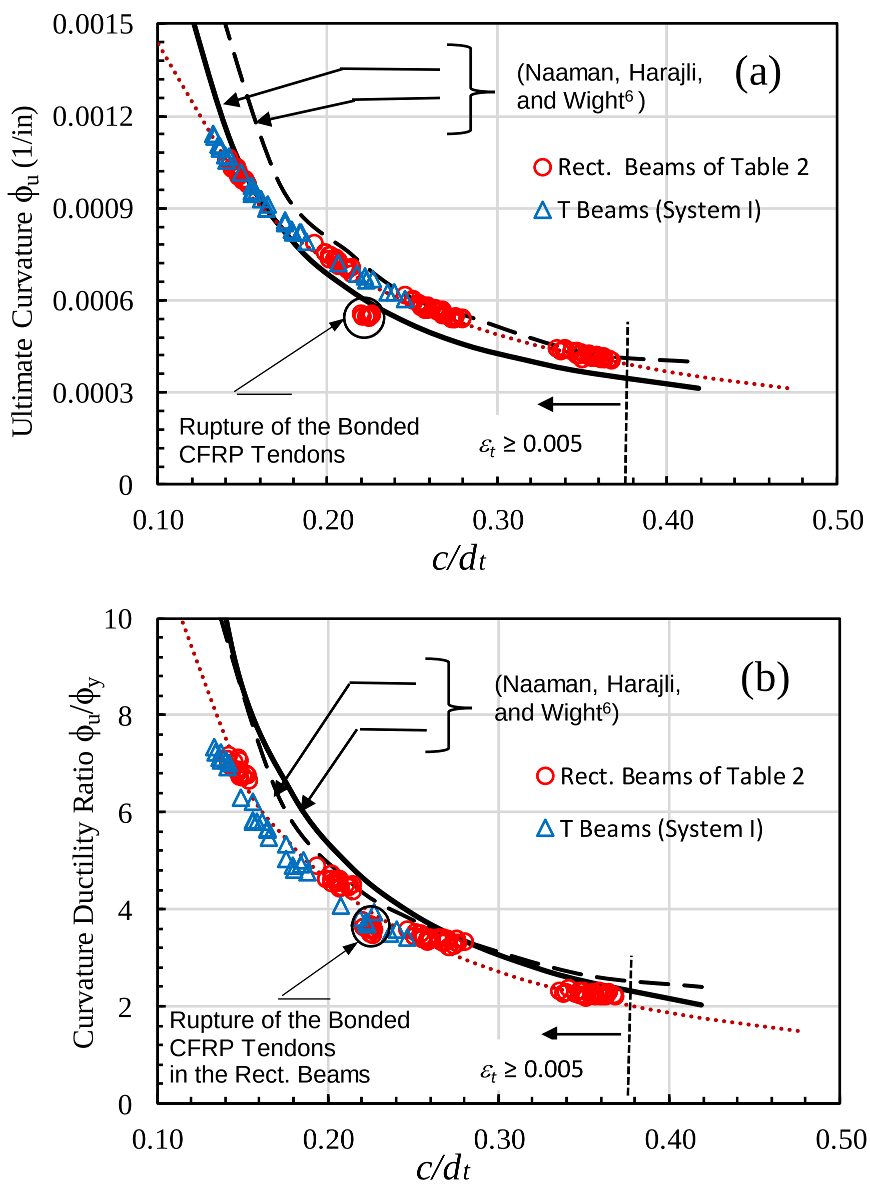

Fig. 9 – Variation of (a) ultimate curvature, and (b) curvature ductility ratio versus c/d_t for the designed beams in hybrid systems I through IV (1 in. = 25.4 mm).